Precipitation of molybdenum carbide in steel: multicomponent diffusion and multicomponent capillary effects

N. Fujita and H. K. D. H. Bhadeshia

Alloy carbides are of considerable importance in the design of steels resistant to creep deformation during service at elevated temperatures. Their formation in ternary or higher order steels involves the diffusion of both substitutional and interstitial solutes. Because these solutes diffuse at vastly different rates, there are difficulties in adopting the theory for diffusion controlled growth in binary alloys. The present work presents a method, developed in the context of molybdenum carbide precipitation in steels, for modelling growth with local equilibrium at the interface while at the same time accounting for capillarity effects. The theory is tested against published experimental data. *MST/4128*

At the time the work was carried out the authors were in the Department of Materials Science and Metallurgy, University of Cambridge, Pembroke Street, Cambridge, CB2 3QZ, UK. Mr Fujita is now with the Nippon Steel Corporation, Shintomi, Futtsu 293–8511, Japan. *Manuscript received 29 May 1998; accepted 22 August 1998.*

Introduction

Many steels contain substitutional solutes which have a strong affinity for carbon or nitrogen. Such steels can be hardened by heat treatment which induces the precipitation of fine alloy carbides. Examples of such carbides include MX, M_2C, M_7C_3, M_6C, and $M_{23}C_6$, where M stands for a mixture of iron and substitutional solute atoms and X stands for interstitial solute atoms.

In practice, the heat treatment has to be at a temperature which is in excess of ~500°C in order to allow the substitutional atoms to diffuse in a reasonable time period, over the dimensions necessary for precipitate growth. Cementite and other transition iron carbides can precipitate by a mechanism which requires only the carbon atoms to diffuse; such carbides can therefore precipitate at temperatures as low as 200°C. As a consequence it is inevitable that iron carbide precipitation must precede that of the alloy carbides. It follows that the steel at first softens as the precipitation of iron carbides removes carbon from solid solution, but begins to harden again as a second reaction occurs in which the alloy carbides start to precipitate at the expense of the less stable iron carbides. It is for this reason that such alloys are called secondary hardening steels.

Secondary hardened steels are of great importance in the manufacture of power plant and in the petrochemical industry where creep must be avoided. Attempts have recently been made to quantify the complicated sequence of precipitation reactions as a function of alloy composition and heat treatment. Since the precipitation reactions involve a large set of reactions often occurring together, Robson and Bhadeshia[1,2] adapted the classical Avrami theory to deal with simultaneous transformations. Such work is of use in the design of new alloys. However, there are a number of fundamental problems which are outside of this framework of simultaneous transformations, associated with the growth of individual phases, which prevent accurate solutions.

PROBLEM 1: MULTICOMPONENT DIFFUSION

A reasonable approximation for isothermal diffusion controlled growth is that the compositions of the phases in contact at the interface are in local equilibrium. It follows that for a binary alloy these compositions are given by a tieline of the equilibrium phase diagram. The concentration profile which develops during the precipitation of a solute rich phase β from a matrix α is illustrated in Fig. 1, where $c^{\alpha\beta}$ is the concentration of solute in α which is in equilibrium with β, and $c^{\beta\alpha}$ is the concentration of solute in β which is in equilibrium with α; both are obtained from the phase diagram. The average solute concentration in the alloy is designated $\bar{c}$.

Solute is removed from the matrix as the precipitate grows but since the temperature is fixed during isothermal transformation, the interface compositions must remain fixed at $c^{\alpha\beta}$ and $c^{\beta\alpha}$ if the local equilibrium is to be maintained. It follows that the rate at which solute is removed from the matrix as the β phase grows must be equal to the flux of solute to the α/β interface

$$v(c^{\beta\alpha} - c^{\alpha\beta}) = -D \left.\frac{\partial c}{\partial z}\right|_{z=z^*} \quad . \ . \ . \ . \ . \ . \ . \ . \ . \ (1)$$

where v is the interfacial velocity, z is the axis along the growth direction, z^* is the position of the interface, and D is the solute diffusion coefficient in the matrix phase. The concentration gradient is evaluated at the position of the interface.

The original work[1] treated the growth of carbides using a binary approximation, i.e. in terms of the diffusion of the substitutional element alone. This is incorrect because the mass balance equation will not be satisfied for the interstitial solute. For a ternary steel containing a metallic solute (M) and carbon (C), there are two such equations which have to be satisfied simultaneously†

$$\begin{aligned} v(c_M^{\beta\alpha} - c_M^{\alpha\beta}) &= -D_M \left.\frac{\partial c_M}{\partial z}\right|_{z=z^*} \\ v(c_C^{\beta\alpha} - c_C^{\alpha\beta}) &= -D_C \left.\frac{\partial c_C}{\partial z}\right|_{z=z^*} \end{aligned} \quad . \ . \ . \ . \ . \ . \ . \ . \ (2)$$

Coates[3] and Kirkaldy[4] realised that because $D_M \ll D_C$, it would in general be impossible to satisfy these equations simultaneously for a tieline passing through $\bar{c}$, apparently implying that growth cannot occur with equilibrium at the interface. However, for a ternary alloy, there is an additional degree of freedom given by the phase rule so that there is a choice of tielines at any given temperature. The local

---

† The equations presented here neglect cross diffusion effects., e.g. the dependence of the flux of carbon on the gradient of M (Refs. 3 and 4). This is considered to be a reasonable approximation in the present context.

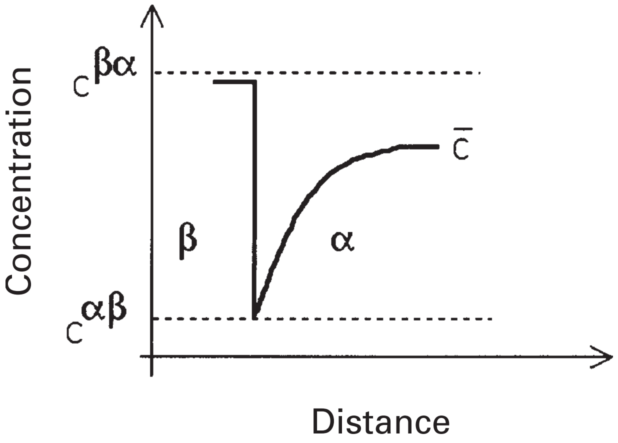

1 Solute concentration profile during diffusion controlled precipitation of β from α

equilibrium condition can be maintained by choosing a tieline which either minimises the concentration gradient of carbon (thus allowing the substitutional solute flux to keep pace) or maximises the gradient of the substitutional solute to compensate for its small diffusivity.

These concepts are well established in treatments of the growth of ferrite from austenite, but as a first approximation were not incorporated in the calculation of carbide precipitation kinetics,[1,2,5] where the diffusion controlled growth was treated essentially as a binary Fe–M problem. Further studies, to be discussed below, have shown that this approximation leads to significant mass balance discrepancies and hence cannot in general be tolerated.

PROBLEM 2: CAPILLARITY

The state of equilibrium between two phases changes with the curvature of the interface separating them. This well established capillarity effect scales with the interfacial energy because additional work has to be done to create a new interfacial area as a curved interface moves. The free energy of a carbide phase varies relatively sharply with deviations from the stoichiometric composition so it can be assumed that the carbide composition is not sensitive to the interface curvature. However, the equilibrium composition of the ferrite changes as follows[6]

$$c_{\mathrm{r}}^{\alpha\beta}=\left(1+\frac{\Gamma}{r}\right)c^{\alpha\beta} \quad . \; . \; . \; . \; . \; . \; . \; . \; . \; . \; . \; . \; . \quad (3)$$

where

$$\Gamma=\frac{\sigma v^{\beta}}{kT}\,\frac{1-c^{\alpha\beta}}{c^{\beta\alpha}-c^{\alpha\beta}}$$

and

$$v\approx\frac{\bar{c}-c_{\mathrm{r}}^{\alpha\beta}}{c^{\beta\alpha}-c_{\mathrm{r}}^{\alpha\beta}}\,\frac{D}{r}$$

where r is the radius of curvature, Γ is a capillarity constant which is directly proportional to the interfacial energy σ, $c^{\alpha\beta}$ is the solute concentration in α which is in equilibrium with β when $r=\infty$, and v^{β} is the molar volume of the β phase. The modified composition $c_{\mathrm{r}}^{\alpha\beta}$ is therefore easy to estimate for a binary alloy. At some critical value, where $r=r_{\mathrm{c}}$ and $c_{\mathrm{r}}^{\alpha\beta}=\bar{c}$, growth ceases.

Equation (3) cannot simply be applied to a ternary alloy with two solutes, bearing in mind that $c_{\mathrm{C}}^{\alpha\beta}$ and $c_{\mathrm{M}}^{\alpha\beta}$ are not independent but are connected by a tieline of the phase diagram. A straightforward application to each solute in turn simply gives two different values of r_{c}, a situation which is not physical since there is only one interface for both solutes. It does not appear from the literature that the problem of multicomponent capillarity within the constraint of local equilibrium has been solved.

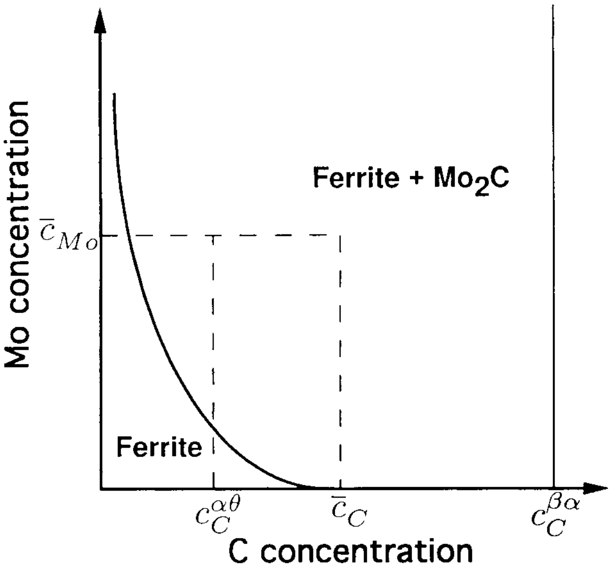

2 Schematic isothermal section through Fe–Mo–C phase diagram showing ferrite and Mo$_2$C phase fields

SUMMARY

Previous work[1,2,5] on the calculation of the kinetics of precipitation reactions in secondary hardening steels has been based on carbide growth in binary Fe–M systems. This was justified by stating that since carbon diffuses rapidly, growth should be controlled by the slower diffusing M atoms. It is now known that this is not a reasonable approximation because it fails to ensure mass balance for all the species of atoms involved in the transformation. The binary approximation is also inappropriate because it leads to different critical tip radii for different solutes.

The aim of the present study was to resolve these difficulties and to test the new methodology using published data for ternary Fe–Mo–C steel which precipitates molybdenum carbides. The framework of the Avrami theory for simultaneous transformations as developed in earlier studies is nevertheless necessary since cementite precipitation must precede that of Mo$_2$C.

Cementite

Cementite precipitation from supersaturated martensite occurs rapidly even at very low temperatures. This is because it forms by a mechanism which does not involve the diffusion of substitutional solutes or iron atoms, just the interstitial carbon atoms. The ratio of iron to substitutional solute atoms does not therefore change during this paraequilibrium[7–9] transformation.

In the context of secondary hardening steels, the time period for cementite precipitation is so small that it can be assumed that the starting microstructure already contains precipitates of cementite. The number density N_{θ} of cementite particles per metre cubed is found experimentally to be given by

$$N_{\theta}=2{\cdot}23\times10^{22}w_{\mathrm{C}}-10^{21} \quad . \; . \; . \; . \; . \; . \; . \; . \; . \quad (4)$$

where w_{C} is the concentration of carbon in wt-%.[10] This empirical equation was established using Fe–0·15C–2·25Cr–1Mo and Fe–0·10C–3Cr–1·5Mo (wt-%) steels, so it may be expected to apply to tempered martensitic steels with carbon concentrations in the range 0·10–0·15 wt-%.

The chemical composition of the cementite adjusts towards equilibrium during the heat treatment needed to induce molybdenum carbide precipitation. This process depletes the matrix of substitutional solute atoms and

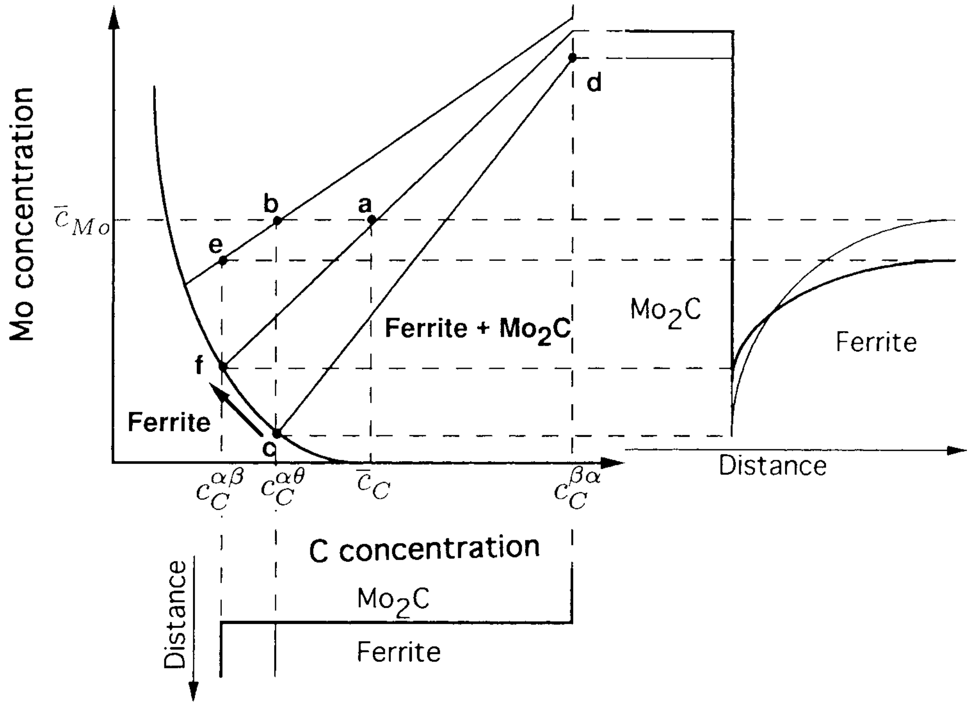

3 Schematic isothermal section through Fe–Mo–C phase diagram showing ferrite and Mo$_2$C phase fields

hence must be taken into account in any model for molybdenum carbide precipitation. The theory for the enrichment of a cementite particle of thickness d has been described by Bhadeshia[11]

$$t_c^{1/2} = \frac{d\pi^{1/2}(\bar{c}-c_\theta)}{4D^{1/2}(c^{\theta\alpha}-\bar{c})} \quad . \; . \; . \; . \; . \; . \; . \; . \; . \; . \; . \; . \; . \; (5)$$

where c_θ is the mean composition of the cementite (designated θ) at time t_c, D is the diffusion coefficient for the solute concerned, and $c^{\theta\alpha}$ is the concentration in θ which is in equilibrium with α. Previous experiments[10] indicate that the thickness of cementite is different when precipitated at the martensite lath boundaries (~50 nm) when compared with that precipitated within the laths (~20 nm). These are the values assumed in the present work and the particles at the boundaries have been modelled as a separate phase from those within the laths. This is straightforward in the framework of simultaneous transformations as described elsewhere.[1,2]

The cementite must eventually begin to dissolve as the precipitation of the thermodynamically more stable Mo$_2$C (β) gathers pace. The dissolution of cementite provides a source of solute for the growing Mo$_2$C. The dissolution for each particle begins when the concentration $c_r^{\alpha\beta}$ becomes less than $c^{\alpha\theta}$, thereby driving the diffusion of solute from the cementite to the Mo$_2$C. The dissolution velocity v_d is given by[1]

$$v_d(c^{\theta\alpha}-c_r^{\alpha\theta}) = D\frac{c^{\alpha\theta}-c_r^{\alpha\beta}}{\bar{d}} \quad . \; . \; . \; . \; . \; . \; . \; . \; . \; . \; (6)$$

where $c_r^{\alpha\beta}$ is the concentration of solute in the ferrite at the interface with a β particle of radius r. The mean distance between the cementite and Mo$_2$C particles $\bar{d}$ is given by[1]

$$\bar{d} = (N_{d\theta}+N_{d\beta})^{-1/3} \quad . \; . \; . \; . \; . \; . \; . \; . \; . \; . \; . \; . \; (7)$$

where $N_{d\theta}$ and $N_{d\beta}$ are the number densities of cementite and Mo$_2$C particles respectively.

The treatment of cementite as presented here is not new but is an essential precursor to Mo$_2$C precipitation which is presented below with solutions to the problems highlighted earlier.

Mo$_2$C precipitation

NUCLEATION

Classical theory[6] is used to estimate the nucleation rate I for Mo$_2$C

$$I = N_\beta \frac{kT}{h}\exp\left(-\frac{G^*+Q^*}{kT}\right) \quad . \; . \; . \; . \; . \; . \; . \; . \; . \; (8)$$

where

$$G^* = \frac{16\pi\sigma^3}{3(\Delta G_v)^2}$$

and N_β is the number density of nucleation sites for Mo$_2$C, h and k are the Planck and Boltzmann constants respectively, Q^* is the activation energy for the transfer of atoms across the nucleus/precipitate interface, assumed to be about half the activation energy for volume diffusion, T is the absolute temperature, ΔG_v is the chemical free energy change per unit volume, and σ is the interfacial energy per unit area.

GROWTH

Figure 2 shows a schematic isothermal section of the Fe–Mo–C phase diagram. The alloy has an average carbon concentration which is $\bar{c}_C$ but the carbon left in solution in the ferrite when cementite has precipitated $c_C^{\alpha\theta}$ is the smaller concentration of carbon which is initially available for the precipitation of Mo$_2$C.

It was stated earlier that there are two ways in which the mass conservation equations for molybdenum and carbon can be satisfied simultaneously. The first is to choose a tieline which greatly increases the gradient of molybdenum to compensate for its low diffusivity. This would require the carbide to have virtually the same molybdenum concentration as the matrix with very little partitioning of molybdenum, but with a sharp concentration spike at the interface in order to maintain local equilibrium.[3,4] This situation is only possible with very large driving forces.[3,4] The case of secondary hardening steels refers, on the other hand, to precipitation at low supersaturations. In these circumstances, the only alternative is to

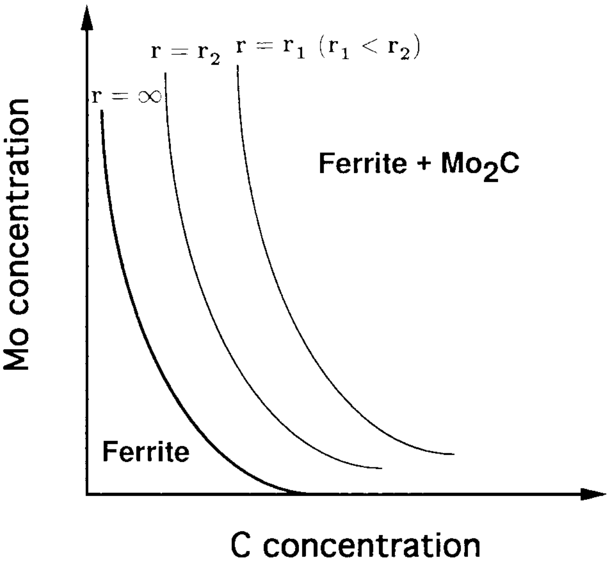

4 Schematic illustration of changes in $\alpha/(\alpha+\mathrm{Mo_2C}\ (\beta))$ phase boundary for given interface curvature values r

choose a tieline which reduces the gradient of carbon to such an extent that the flux of carbon is reduced to a level consistent with that of molybdenum. Following Coates,[3] this can be done by drawing a vertical construction line through the point b in Fig. 3, which represents the composition of the ferrite from which Mo_2C will precipitate. The intersection of the vertical line with the $\alpha/(\alpha+\beta)$ phase field defines completely the tieline which fixes the interface compositions in a manner which satisfies the two mass conservation conditions simultaneously because the large diffusion coefficient of carbon is compensated for by the very small concentration gradient of carbon.[3,4] Note that this also maintains local equilibrium at the interface since the compositions at the interface (given by the points c and d for α and β respectively) are connected by a tieline in the phase diagram.

TIELINE SHIFTING

The precipitation of Mo_2C must deplete the solute concentration in the matrix. The locus of the matrix composition at any instant is along the direction b → e (Fig. 3). Any change in the matrix composition also leads to a different choice of tieline, the locus of $c^{\alpha\beta}$ being along c → f. This tieline shifting[3] continues until the reaction stops when the tieline intersects the average composition a and $c^{\alpha\beta}=\mathrm{f}$ in Fig. 3.

CAPILLARITY

The method developed here to account for the capillarity effect in a ternary alloy involves the calculation of the $\alpha/(\alpha+\mathrm{Mo_2C}\ (\beta))$ boundary on the isothermal section of the phase diagram, as a function of the curvature of the

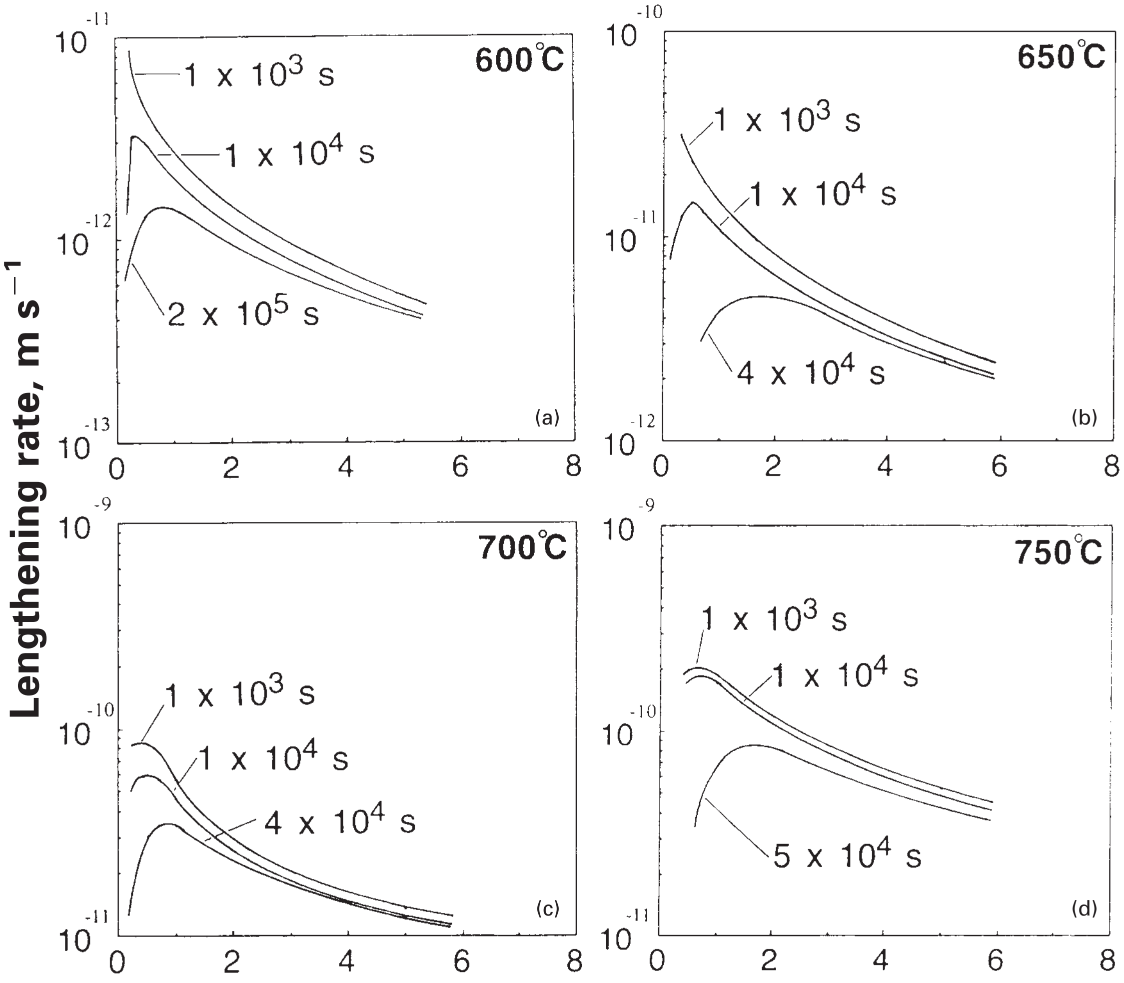

5 Calculated growth rates of Mo_2C as function of needle tip radius and transformation time at given temperatures for Fe–2Mo–0·1C steel

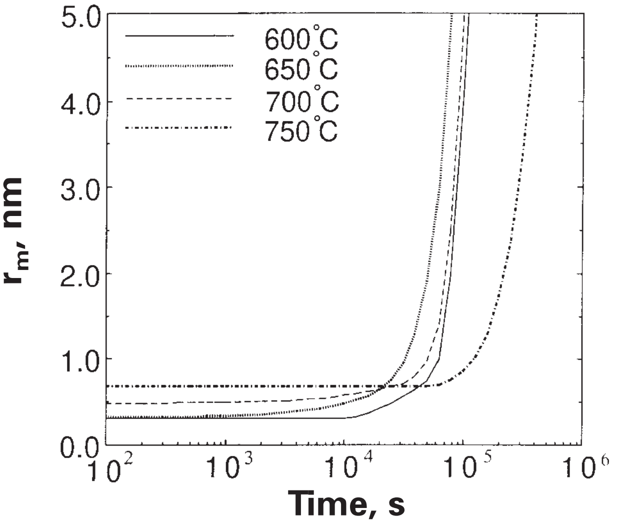

6 Calculated needle tip radius r_m corresponding to maximum growth rate as function of transformation time and temperature for Fe–2Mo–0·1C steel

interface r. Equation (3) is used to calculate $c^{\alpha\beta}_{r,\mathrm{C}}$ and $c^{\alpha\beta}_{r,\mathrm{Mo}}$ for a fixed value of the interface radius of curvature r. The growth velocity is then calculated using the method described in the previous section but with the curvature modified phase boundary (Fig. 4).

In this way, the interface velocity can be plotted as a function of the radius r; such a function must go through a maximum because a large radius approximates to one-dimensional diffusion confined to regions normal to the interface, whereas the capillarity effect reduces the velocity as $r \rightarrow r_c$. The maximum velocity can then be assumed to correspond to the actual growth velocity, an assumption known as the Zener hypothesis.[12]

This procedure solves all the problems described in the introduction. It deals correctly with mass balance for both the diffusing species and the capillarity corrected concentrations for each solute give the same tip radius when inserted into equation (3). Before describing the results obtained using this method it is necessary to summarise the procedure[1] used to deal with soft impingement.

SOFT IMPINGEMENT

The changes in the chemical composition of the matrix during precipitation are vital to the development of the precipitation process. Composition gradients develop in the ferrite and the gradients originating from different particles eventually interfere, changing the rate equations. This is taken into account using the so called mean field approximation in which the changes are averaged out over the residual matrix.[1] The far field matrix composition seen by each precipitate is this averaged composition denoted $\bar{c}'$

$$\bar{c}' = \bar{c} - \frac{V_\theta(c^{\theta\alpha} - \bar{c}) + V_\beta(c^{\beta\alpha} - \bar{c})}{1 - V_\theta - V_\beta} \qquad (9)$$

where V_i is the volume fraction of the ith phase.

The effect of soft impingement in the mean field approximation may also be expressed in terms of an extent of reaction parameter with the dimensionless

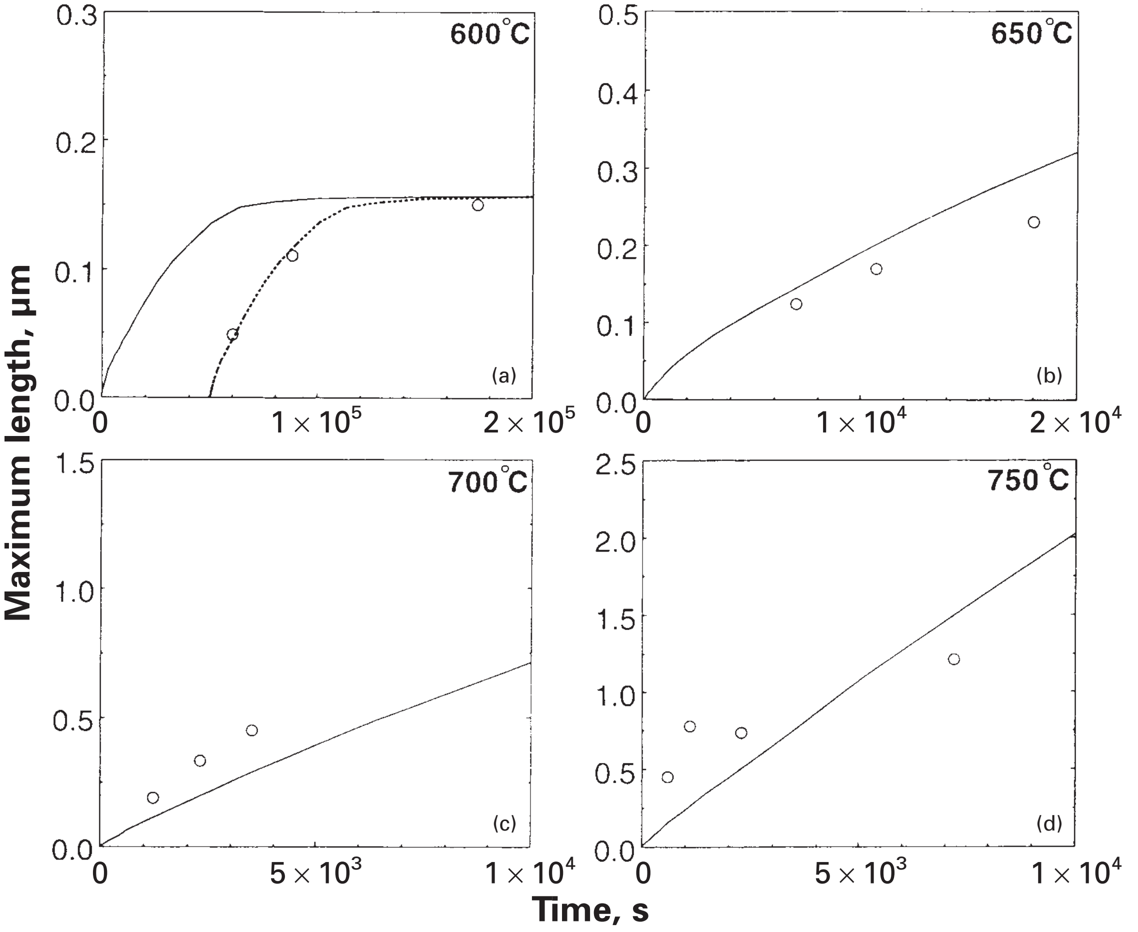

○ experimental data by Hall *et al.*[5]

7 Comparison of calculated and measured particle dimensions as function of time and temperature for Fe–2Mo–0·1C steel

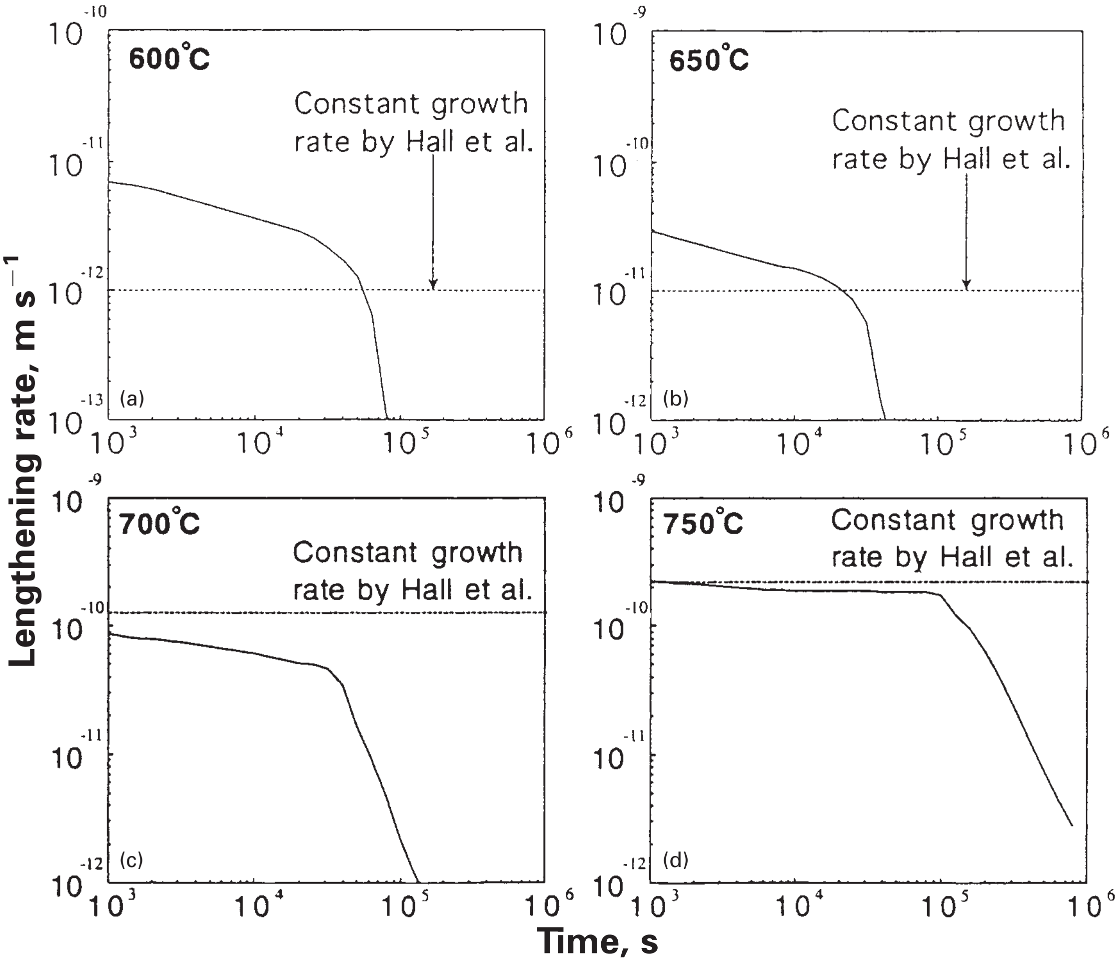

8 Calculated lengthening rate of Mo$_2$C as function of time and temperature for optimum N_β values for Fe–2Mo–0·1C steel: constant growth rate after Ref. 5

supersaturation

$$\Phi=\frac{f}{f_{\max}} \quad . \; . \; . \; . \; . \; . \; . \; . \; . \; . \; . \; . \; . \; . \; . \; . \; . \quad (10)$$

where

$$f_{\max}=\frac{\bar{c}-c^{\alpha\beta}}{c^{\beta\alpha}-c^{\alpha\beta}}$$

and f is the instantaneous fraction and $f_{\max}$ is the maximum fraction of a given phase. The function Φ ranges from 0 to 1 and represents the fraction of excess solute remaining in the matrix relative to the equilibrium composition of the precipitate. It is assumed that the chemical driving force for precipitation is linearly related to Φ

$$\Delta G_{\mathrm{i}}=(1-\Phi_{\mathrm{i}})\Delta G_{\mathrm{i}}^{0} \quad . \; . \; . \; . \; . \; . \; . \; . \; . \; . \; . \quad (11)$$

where $\Delta G_{\mathrm{i}}^{0}$ is the driving force available before any precipitation of phase i.

Similar changes owing to the enrichment of cementite can also be dealt with by defining

$$\Phi_{\theta}=\frac{c-\bar{c}'}{c^{\theta\alpha}-\bar{c}'} \quad . \; . \; . \; . \; . \; . \; . \; . \; . \; . \; . \; . \; . \; . \quad (12)$$

Comparison with published data

The lengthening rate of Mo$_2$C particles in tempered martensite has been measured by Hall *et al.*[5] for a variety of temperatures in an alloy of composition Fe–2Mo–0·1C, wt-%. The rate is determined by measuring the length of the largest particle observed for a particular isothermal heat treatment time. Such data are then plotted as a function of time to estimate the lengthening rate. The original data were analysed assuming that it is only the diffusion of molybdenum which determines the lengthening rate of the Mo$_2$C needles; the growth rate was also assumed to be constant throughout the heat treatment.

Example calculations were carried out using the multicomponent model described earlier, beginning with a microstructure consisting of paraequilibrium cementite and ferrite in which Mo$_2$C eventually grows at the expense of the cementite. The calculations are therefore in the framework of the simultaneous transformation model* (Ref. 1); this means that all transformations (cementite enrichment, Mo$_2$C precipitation) begin at the same time but occur in this case at vastly different rates. Furthermore, the dissolution of cementite occurs naturally in this framework when the mean composition of the matrix falls below that consistent with its equilibrium with cementite, as Mo$_2$C formation withdraws solute from the ferrite. Because of the multicomponent mass balance conditions inherent in the present form of the simultaneous transformations model, the dissolution of cementite occurs at a rate consistent with the precipitation of Mo$_2$C; this was not the case in the earlier work.[1] The number density of Mo$_2$C nucleation sites was taken to be $1{\cdot}5\times10^{15}$ m^{-3} and the Mo$_2$C/α interfacial energy was set at 0·2481 J m^{-2} (Ref. 13).

The results are presented in Fig. 5. The Mo$_2$C grows in the form of needles so the lengthening rate is a function of

---

* The Avrami theory has recently[1] been adapted to treat the precipitation of more than one phase at a time. This simultaneous transformation framework is essential in order to allow interactions between cementite and alloy carbides.

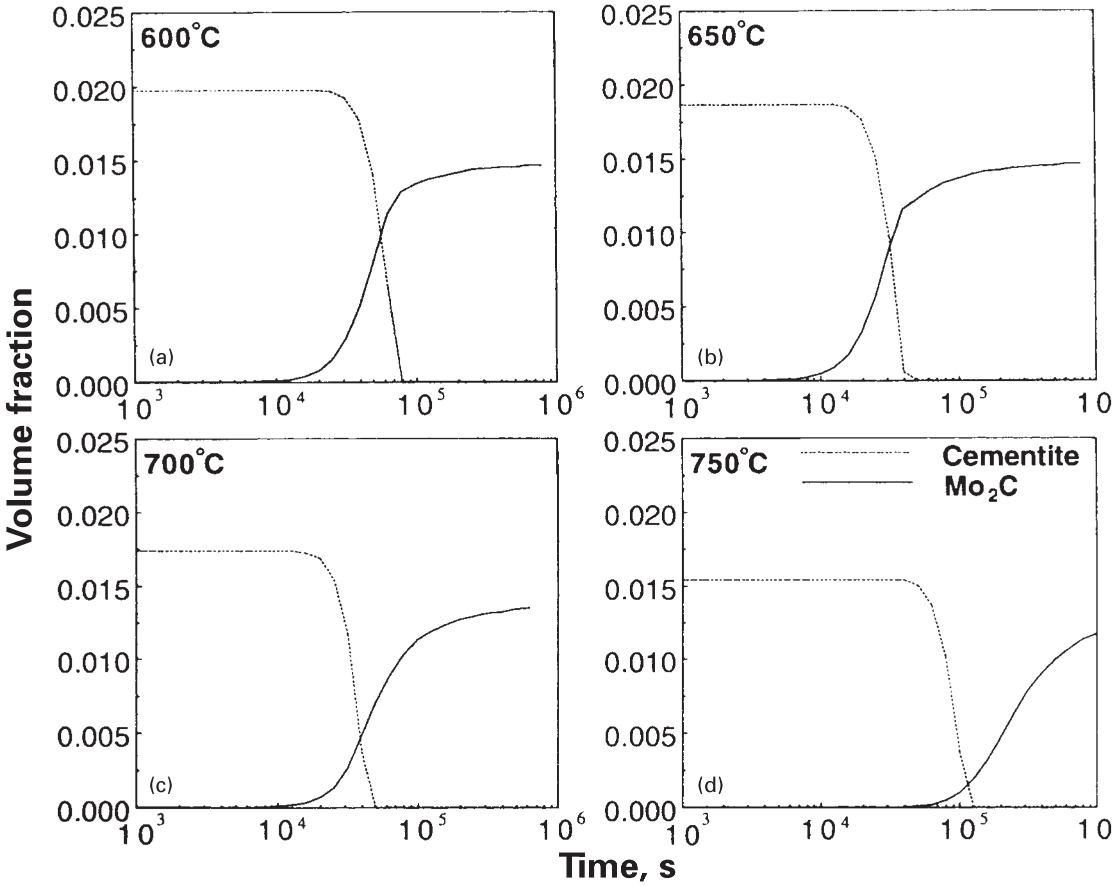

9 **Calculated fractions of cementite and Mo_2C as function of time and temperature for optimum N_β values for Fe–2Mo–0·1C steel**

the tip radius. In each case the growth rate goes through a maximum which is assumed to correspond to the actual growth rate at any instant of time in the present work. Notice also that the rate changes substantially with time because of soft impingement and the associated tieline shifting.

The radius r_m corresponding to the maximum velocity increases with time because the driving force for transformation decreases with the progress of precipitation (Fig. 6). For the same reason, at a fixed heat treatment time at an early stage, r_m also increases with the transformation temperature. Table 1 gives the parameters used to calculate the curves plotted in Figs. 6–9.

The number density N_β of Mo_2C nucleation sites is important in the calculation but is unknown. This makes a complete comparison with the data of Hall *et al.*[5] impossible. Nevertheless, the trends in the lengthening rate data can be predicted if N_β is taken to be an adjustable parameter. Changing N_β can only affect the lengthening rate when soft impingement between particles nucleated at different locations becomes important; it should not therefore affect the initial lengthening rate.

It is apparent from Fig. 7 that there is a rather good detailed agreement between the experimental data and the calculations. Figure 7*a* shows the results for 600°C; the dashed curve represents the raw experimental data and the curve for $N_\beta = 1{\cdot}5 \times 10^{15}$ m^{-3} emulates the data extremely well apart from the shift along the time axis.

The growth rate is the slope of the curve and is shown in Fig. 8, as is the great reduction in rate owing to soft impingement as the volume fraction evolves (Fig. 9). This is in contrast to the original analysis where a straight line of best fit is fitted to the whole set of isothermal data to derive a constant growth rate. Thus, the agreement between the constant growth rate derived by Hall *et al.*[5] and the initial rate calculated (Fig. 8) is best at 750°C, since soft impingement effects do not occur within the time scale of their experiments ($< 10^4$ s).

Table 1 Parameters used in calculations for Fe–2Mo–0·1C steel[13,14]

Parameter	Value used in calculations
Interfacial energy	$0{\cdot}2481$ J m^{-2}
Diffusion coefficient	$1{\cdot}1 \times 10^{-4}$ m^2 s^{-1}
Activation energy for diffusion	240×10^{-4} J m^{-2}

Discussion

The calculations basically showed good agreement with experimental data even though there are no significant adjustable parameters other than N_β (Fig. 7). Note that the interfacial energy σ is from earlier work where its value has to fit into a ranking consistent with observed precipitation sequences. The agreement is, as expected, best when a comparison is made with the rate calculated for the early stages of transformation.

Table 2 Equilibrium phases in Fe–2Mo–0·1C steel for each temperature calculated using MTDATA[15]

Temperature, °C	Equilibrium phases
600	Ferrite, $M_{23}C_6$, and M_6C
650	Ferrite, $M_{23}C_6$, and M_6C
700	Ferrite, $M_{23}C_6$, and M_6C
750	Ferrite and M_6C

Table 2 gives the equilibrium phases for each temperature calculated using MTDATA,[15] which is a phase diagram calculation program. The equilibrium phases in the steel analysed include $M_{23}C_6$ and M_6C, but were not observed by Hall *et al.*,[5] presumably because of the short time scales of the heat treatments. This sequence of alloy carbide formation is typical of secondary hardening steels. The formalism developed here to deal with multicomponent diffusion and capillarity will in future be developed to deal with the simultaneous precipitation of more than one alloy carbide.

Conclusion

A methodology has been developed to deal with the growth of molybdenum carbide in a ternary alloy, taking proper account of mass balance during diffusion controlled growth while at the same time dealing with multicomponent capillarity effects. The method has been satisfactorily validated against published experimental data.

Acknowledgements

The authors are grateful to the Nippon Steel Corporation for funding this research and to Professor Alan Windle for the provision of laboratory facilities at the University of Cambridge.

References

1. J. D. ROBSON and H. K. D. H. BHADESHIA: *Mater. Sci. Technol.*, 1997, **13**, 631.
2. J. D. ROBSON and H. K. D. H. BHADESHIA: *Mater. Sci. Technol.*, 1997, **13**, 640.
3. D. E. COATES: *Metall. Trans.*, 1973, **4**, 2313.
4. J. S. KIRKALDY: *Can. J. Phys.*, 1958, **36**, 907.
5. M. G. HALL, K. R. KINSMAN, and H. I. AARONSON: *Metall. Trans.*, 1972, **3**, 1320.
6. J. W. CHRISTIAN: 'Theory of transformation in metals and alloys', 2nd edn, Part 1, 181, 418; 1975, Oxford, Pergamon.
7. A. HULTGREN: *Trans. ASM*, 1947, **39**, 915.
8. E. RUDBERG: *Jernkontorets Ann.*, 1952, **136**, 91.
9. H. I. AARONSON and H. A. DOMIAN: *Trans. AIME*, 1966, **236**, 781.
10. N. FUJITA and H. K. D. H. BHADESHIA: in Proc. Conf. on 'Advanced heat resistant steels for power generation', San Sebastian, Spain, April 1998, The Institute of Materials.
11. H. K. D. H. BHADESHIA: *Mater. Sci. Technol.*, 1989, **5**, 131.
12. C. ZENER: *Trans. AIME*, 1946, **167**, 550.
13. J. D. ROBSON and H. K. D. H. BHADESHIA: *Calphad*, 1996, **20**, 447.
14. J. FRIDBERG, L.-E. TORNDAHL, and M. HILLERT: *Jernkontorets Ann.*, 1969, **153**, 263.
15. S. M. HODSON: Metallurgical and Thermochemical Databank (MTDATA), National Physical Laboratory, Teddington, UK, 1989.